Wind Energ. Sci. Discuss., doi:10.5194/wes-2017-1, 2017
Manuscript under review for journal Wind Energ. Sci.
Published: 6 February 2017

eawe european academy of wind energy
Open Access WIND ENERGY SCIENCE DISCUSSIONS

3D Shear layer simulation model for the mutual interaction of wind turbine wakes: Description and first assessment

Davide Trabucchi, Lukas Vollmer, and Martin Kühn
ForWind - University of Oldenburg, Institute of Physics, Küpkersweg, 70, 26129 Oldenburg, Germany
Correspondence to: Davide Trabucchi (davide.trabucchi@uni-oldenburg.de)

Abstract. The number of turbines installed in offshore wind farms has strongly increased in the last years and at the same time the need for more precise estimation of the wind farm efficiency. In this sense, the interaction between wakes has become a relevant aspect for the definition of a wind farm layout, for the assessment of its annual energy yield and for the evaluation of wind turbine fatigue loads. For this reason, accurate models for multiple wakes are a main concern of the wind energy community. Existing engineering models can only simulate single wakes which are superimposed when they are interacting in a wind farm. This method is a practical solution, but it is not fully supported by a physical background. The limitation to single wakes is given by the assumption that the wake is axisymmetric. As alternative, we propose a new shear layer model which is based on the existing engineering wake models, but is extended to simulate also non-axisymmetric wakes. In this paper, we present the theoretical background of the model and two application cases. First, we proved that for axisymmetric wakes the new model is equivalent to a commonly used engineering model. Then, we evaluated the improvements of the new model for the simulation of multiple wakes using large eddy simulations as reference. In particular, we report the improvements of the new model in comparison to a sum-of-squares superposition approach for the simulation of three interacting wakes. The remarkable lower deviation from the reference in terms of rotor equivalent wind speed considering two and three interacting wakes encourages the further development of the model, and promises a successful application for the simulation of wind farms.

1 Introduction

When the wind passes through the wind turbine rotor, kinetic energy is extracted from the wind and is converted into electrical power. This process generates a wake which propagates downstream. Wakes can be described as shear flows with lower speed and higher turbulent fluctuations than in front of the rotor. In this sense, wakes are the main cause of power losses in wind farms (Walker et al., 2016). Besides that, wakes hitting a turbine contribute to the increase in the fatigue loads of its components. For these reasons, wake modeling plays a major role in the definition of the layout of wind farms, in the evaluation of their annual energy yield and in the estimation of the lifetime of wind turbine components. Consequently, more accurate wake models can indirectly contribute to the cost-of-energy reduction due to more tailored design of wind turbines and wind farms.

Despite the large progress especially in the numerical modelling, Vermeer et al. (2003) still provide a comprehensive review about traditional wake modeling. Most of the engineering models described in their work evaluate the wind field of a single

Wind Energ. Sci. Discuss., doi:10.5194/wes-2017-1, 2017
Manuscript under review for journal Wind Energ. Sci.
Published: 6 February 2017

eawe european academy of wind energy
Open Access WIND ENERGY SCIENCE DISCUSSIONS

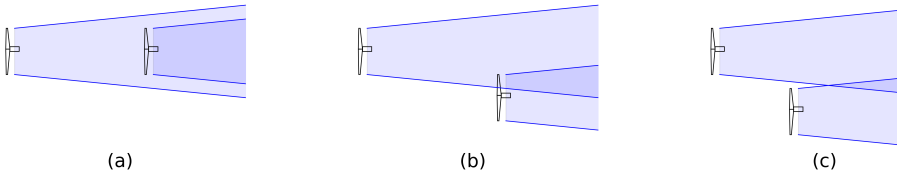

Figure 1. Different cases of merging wakes: (a) Aligned wakes (b) Wake-turbine interaction (c) Wake-wake interaction.

wake and combine the individual results in case of mutual interaction. More sophisticated Computational Fluid Dynamics (CFD) such as Reynolds Average Navier-Stokes (RANS) or Large Eddy Simulations (LES) can deal with wake superposition better and provide more realistic results. However, these alternatives have a much higher computational cost and therefore can become prohibitive for commercial applications.

Commercial codes for estimating wake effects in a wind farm often implement the steady state, axisymmetric shear layer approximation of the RANS equations, e.g. the one used in the Ainslie model (Ainslie, 1988). Due to the axial symmetry assumption, only the wind deficit of single wakes or wakes aligned on the same axis as those illustrated in Fig. 1a can be simulated with such models. For the case of wake-turbine or wake-wake interaction of Fig. 1b and c pragmatic methods are required. In the kinematic model by Katic et al. (1986), the square addition of the individual wake deficits is applied to overcome this limitation and to be able to deal with multiple wakes. In a previous study, Lissaman (1979) proposed their linear addition, however this method tends to overestimate the velocity deficit and could lead to unrealistic flow reversal when many wakes merge.

Machefaux (2015) compared the performance of the linear approach with the square wake addition approach and noticed that the former is to be preferred for wakes of turbines operating at a low thrust coefficients, while the latter returns better results in the opposite case. From this observation, he developed a wake superposition model which combines the linear and square addition of single wakes using a weighted average depending on the thrust on the rotor.

Crespo et al. (1999) declared that the classical wake superposition methods does not rely on a physical background and, if not handled properly, could lead to unrealistic results. This statement gives the motivation of this paper. Herewith, we aim to describe the 3D shear layer (3DSL) model, that is an innovative engineering model able to deal with the superposition of wakes and based on physical principles without relying on an addition method. Moreover, this study aims to verify the consistency of the model with other axisymmetric models. Finally, the performances of the single wakes square addition approach and of the direct simulation of interacting wakes with the 3DSL model are assessed against the wind fields extracted from the LES of the same wake conditions. The rotor equivalent wind speed (REWS) is the figure of merit of the assessment.

Wind Energ. Sci. Discuss., doi:10.5194/wes-2017-1, 2017
Manuscript under review for journal Wind Energ. Sci.
Published: 6 February 2017

eawe european academy of wind energy
Open Access WIND ENERGY SCIENCE DISCUSSIONS

2 Model description

In the following the theoretical background of the 3DSL model is provided along with the description of its numerical implementation. Moreover, it is explained how to evaluate the parameters needed to apply the model.

2.1 The mathematical definition

The 3DSL model implements a shear layer approximation of the steady RANS equations following the approach described by Lange et al. (2003). It is intended to model the wind turbine wake deficit u_D defined as

$$u_D = \frac{u_w}{u_i} \tag{1}$$

using the inflow wind speed u_i and the wake wind speed u_w. The 3DSL model is valid starting from a downstream distance where the pressure gradient in the stream-wise direction is negligible. Moreover, the viscous term is not considered and no external forces are applied.

Differently from other existing shear layer models, the 3DSL approach is not formulated in a polar coordinate system, but considering a Cartesian frame of reference, i.e. the stream-wise deficit u_D, the cross-stream and vertical wind components v and w are defined along the x, y and z axis respectively. Considering a dimensional analysis (Cebeci and Cousteix, 2005) the steady RANS equation for flows with a shear layer along the cross-stream and vertical component can be simplified to

$$\begin{cases} \frac{\partial u_D}{\partial x} + \frac{\partial v}{\partial y} + \frac{\partial w}{\partial z} &= 0 \\ u_D \frac{\partial u_D}{\partial x} + v \frac{\partial u_D}{\partial y} + w \frac{\partial u_D}{\partial z} &= -\left(\frac{\partial \overline{u'v'}}{\partial y} + \frac{\partial \overline{u'w'}}{\partial z} \right) \\ \frac{\partial p}{\partial y} = \frac{\partial p}{\partial z} &= 0 \end{cases} \tag{2}$$

The shear stress terms on the right hand side of the second line of Eq. (2) can be modelled by means of an eddy viscosity closure introducing the eddy viscosities ϵ_y, ϵ_z and multiplying them by the corresponding cross-stream and vertical gradients of u:

$$\begin{aligned} \overline{u'v'} &= -\epsilon_y \frac{\partial u_D}{\partial y} \\ \overline{u'w'} &= -\epsilon_z \frac{\partial u_D}{\partial z} \end{aligned} \tag{3}$$

Further details on the eddy viscosity model are provided in Sect. 2.3.

At this point, the system of Eq. (2) is still underdeterminated. To balance the unknown variables and the equations, we assume that the wind components v and w define a conservative vector field in all the cross-sections $y-z$. A potential function Φ can therefore be defined such that

$$\begin{cases} \frac{\partial \Phi}{\partial y} &= v \\ \frac{\partial \Phi}{\partial z} &= w \end{cases} \tag{4}$$

Concerning multiple wakes, this assumption does not imply any limitation since the vector field resulting from the superposition of conservative vector fields is still conservative. However, this assumption limits the domain of possible solutions. For instance,

Wind Energ. Sci. Discuss., doi:10.5194/wes-2017-1, 2017
Manuscript under review for journal Wind Energ. Sci.
Published: 6 February 2017

eawe european academy of wind energy
Open Access WIND ENERGY SCIENCE DISCUSSIONS

swirling wakes in which the tangential velocity is inversely proportional to the distance from the rotation axis are accepted, while wakes rotating as a rigid body are not.

The hypothesis of a potential flow is implicit in the axial symmetry imposed by Ainslie. His model he considers a cylindrical coordinate system defined by the radial coordinate r, the angular coordinate θ and the horizontal coordinate x. The corresponding velocity vector field $\overline{V}(r,\theta,x) = (v_r, v_\theta, u)$ is conservative only if $\nabla \times \overline{V} = 0$. Considering the individual cross-section planes at a certain x coordinate, it implies that $\partial v_r/\partial\theta - \partial v_\theta/\partial r = 0$. This equation is always satisfied by the Ainslie model in which the tangential velocity v_θ is neglected and radial velocity v_r is the same at each radius r.

Thanks to Eq. (4) and considering that $\partial u/\partial x$ depends only on y and z at each vertical cross-section, the conservation of mass (Eq. (2), first line) can be expressed as

$$\frac{\partial^2\Phi}{\partial y^2} + \frac{\partial^2\Phi}{\partial z^2} = g(y,z) \tag{5}$$

where $g(y,z) = -\partial u_D/\partial x$. This formulation is a second order elliptic partial differential equation of the Poisson type, which can be solved numerically.

Considering the aforementioned assumptions, the final formulation of the 3DSL model can be summarised as

$$\begin{cases} \frac{\partial^2\Phi}{\partial y^2} + \frac{\partial^2\Phi}{\partial z^2} &= g(y,z) \\ g(y,z) &= -\frac{\partial u_D}{\partial x} \\ \frac{\partial\Phi}{\partial y} &= v \\ \frac{\partial\Phi}{\partial z} &= w \\ u_D\frac{\partial u_D}{\partial x} + v\frac{\partial u_D}{\partial y} + w\frac{\partial u_D}{\partial z} &= \epsilon_y\frac{\partial^2 u_D}{\partial y^2} + \epsilon_z\frac{\partial^2 u_D}{\partial z^2} \end{cases} \tag{6}$$

2.2 The numerical implementation

The 3DSL model is implemented using finite difference schemes to obtain the numerical formulation of the physical model defined in Eq. (6). On the vertical cross-sections $y-z$, the grid points are equally spaced, while the downstream step size along the x axis is evaluated at each cross-section. This is needed to accomplish the stability constraints of the numerical solution.

The numerical problem can be solved iteratively for well defined initial and boundary conditions. The former are evaluated using a near wake model to calculate the stream-wise deficit at the outlet of the induction zone of the rotor, i.e. where the stream-wise pressure gradient is negligible. The latter are assigned in two different ways: Periodic boundary conditions are applied for the solution of the Poisson equation (Eq. (6), first line) on the lateral, top and bottom boundaries of the computational domain. Differently, for the stream-wise momentum balance (Eq. (6, fifth line) u_D is set as in the initial conditions on the same boundaries. Furthermore, the ground effects are reproduced by imposing $\partial\Phi/\partial z = 0$ on the lower boundary of the domain.

Wind Energ. Sci. Discuss., doi:10.5194/wes-2017-1, 2017
Manuscript under review for journal Wind Energ. Sci.
Published: 6 February 2017

eawe european academy of wind energy
Open Access WIND ENERGY SCIENCE DISCUSSIONS

2.3 Eddy viscosity model

In the 3DSL model, the eddy viscosity is evaluated as

$$\epsilon_{y,z} = \frac{F(x)\, k\, r_{y,z}(x)\, u_{a\,y,z}(x)}{\Phi_m(z_H/L_{MO})} + \kappa\, u_*\, z_H \tag{7}$$

following the approach suggested by Lange et al. (2003) who combines the contribution of the wake (first addend) and of the atmosphere (second addend).

The parameters describing the wake contribution to the eddy viscosity are the empirical parameter $k = 0.015$ and the filter function

$$F(x) = \begin{cases} 0.65 + \left[\left(\frac{x-4.5}{23.32}\right)^{1/3}\right] & x \leq 5.5\, D \\ 1 & x > 5.5\, D \end{cases} \tag{8}$$

which are included to modulate the development of the turbulence generated by the shear layer within the wake deficit (Ainslie, 1988). Last, the parameters $r_{y,z}(x)$ and $u_{a\,y,z}(x)$ are meant to represent the characteristic length and velocity turbulence scales of the wake deficit.

The parameters appearing in Eq. (7) to model the effect of the atmospheric conditions on the eddy viscosity are the momentum flux profile $\Phi_m(z_H/L_{MO})$ as function of the wind turbine hub height z_H and of the Monin-Obukonov length L_{MO} (Dyer, 1974), the Von Karman constant κ and the friction velocity u_*. In a neutrally stratified atmosphere, u_* is proportional to the standard deviation of the stream-wise wind velocity (Panofsky and Dutton, 1984). Referring to experimental data (Panofsky and Dutton, 1984; Lange, 2002), it can be approximated with

$$u_* = \frac{u_{H_{std}}}{2.4} = \frac{TI u_H}{2.4} \tag{9}$$

where u_H, $u_{H_{std}}$ and TI are the inflow velocity at hub height, its standard deviation and the corresponding ambient turbulence intensity.

2.4 Wake characteristic turbulence scales

In the 3DSL model, the representative wake deficit radii in the y and z directions are regarded as the characteristic turbulence length scales r_y and r_z in the corresponding directions. To evaluate r_y and r_z, we average all the values of the wake deficit corresponding to the same y or z respectively. Then, we define the wake width in the y and z directions as the cumulative width where the wake deficit is below 0.1 %. Finally, we consider the radius r_y (r_z) as half of the resulting width.

On each cross-section, we define a local characteristic turbulence velocity scale $u_{a\,y,z}$ as a function of the position $P = (x, y, z)$. For this purpose, the local characteristic velocity scale is derived with the classic turbulence mixing length theory (Pope, 2000), similarly as in the model by Keck et al. (2012). Accordingly, the turbulent velocity scales are modelled by means of the local strain rates of the wake deficit $u'_y(P) = \left.\frac{\partial u}{\partial y}\right|_P$ and $u'_z(P) = \left.\frac{\partial u}{\partial z}\right|_P$ together with the turbulence length scale $r_{y,z}(x)$ in the considered direction:

$$u_{a\,y,z}(P) = u'_{y,z}(P)\, r_{y,z}(x) \tag{10}$$

Wind Energ. Sci. Discuss., doi:10.5194/wes-2017-1, 2017
Manuscript under review for journal Wind Energ. Sci.
Published: 6 February 2017

eawe european academy of wind energy
Open Access WIND ENERGY SCIENCE DISCUSSIONS

Finally we introduce the eddy viscosity factor

$$f_{y,z}(P) = F(x) u'_{y,z}(P)\, r^2_{y,z}(x) \tag{11}$$

which will be useful in the discussion of the results and allows to rewrite Eq. (7) as

$$\epsilon_{y,z}(P) = \frac{k\, f_{y,z}(P)}{\Phi_m(z_H/L_{MO})} + \kappa\, u_*\, z_H \tag{12}$$

2.5 The near wake initialization

To run 3DSL model simulation it is necessary to initialise it with the wind field outside the induction zone of the rotor, because the 3DSL model is not valid directly in the near field behind the rotor as explained in Sect. 2.1.

Werle (2015) and Madsen et al. (2010) suggested possible methodologies suitable for this purpose. Here, we apply a classic disk actuator approach (Burton et al., 2011). We consider a stream tube defined by the cross-sections in the inflow, at the rotor and at the outlet of the induction zone. We indicate the corresponding diameters as D_i, D_r and D_o respectively and we use the same notation for the rotor equivalent wind speed (REWS) U_{RE} (i.e. the average wind speed on the rotor plane) and the stream-wise wind component u. The induction factor a is derived from the evolution of U_{RE} across the stream tube as

$$a = 1 - \frac{U_{RE,r}}{U_{RE,i}} = \frac{1}{2}\left(1 - \frac{U_{RE,o}}{U_{RE,i}}\right) \tag{13}$$

In the calculation of the near wake, first we apply an iterative process to estimate $U_{RE,i}$ until the convergence of D_i: We calculate $U_{RE,i}$ averaging the wind speed u_i on the inflow cross-section D_i. For the first iteration D_i is approximated to the rotor diameter D_r. From the thrust coefficient C_T corresponding to $U_{RE,i}$ we calculate the induction factor

$$a = \frac{1}{2}\left(1 - \sqrt{1 - C_T}\right) \tag{14}$$

and we use it together with the conservation of the mass flow within the stream tube to calculate the new estimation of D_i:

$$D_i = D_r \sqrt{(1-a)} \tag{15}$$

A new $U_{RE,i}$ is then calculated from the new D_i at each iteration step. Once the convergence is reached, the corresponding induction factor is applied to u_i on the inflow cross-section which is then expanded to match the outlet cross-section applying the conservation of mass to the stream lines within the stream tube

$$\begin{aligned} u_o &= u_i\,(1-2a) \\ D_o &= D_r \frac{\sqrt{(1-a)}}{\sqrt{(1-2a)}} \end{aligned} \tag{16}$$

Finally the initial deficit u_{nw} at the near wake outlet is given replacing u_w by u_o in Eq. 1.

2.6 Multiple wakes

The 3DSL model is meant to improve the simulation of wakes interacting in a wind farm replacing the superposition methods usually applied (e.g. the linear or squared addition) by the simulation of all the wakes at once based on a less approximated physical model.

Wind Energ. Sci. Discuss., doi:10.5194/wes-2017-1, 2017
Manuscript under review for journal Wind Energ. Sci.
Published: 6 February 2017

eawe european academy of wind energy
Open Access WIND ENERGY SCIENCE DISCUSSIONS

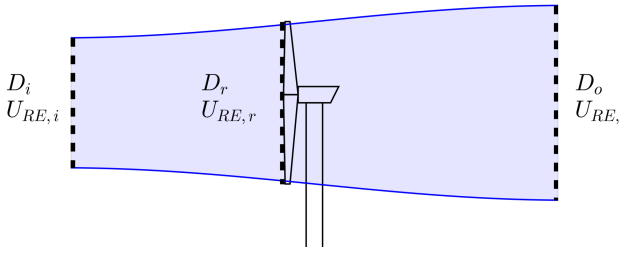

Figure 2. Sketch of the stream tube used to describe the disc actuator approach. The dashed lines represent the inflow, rotor and outlet cross-section which are indicated with the subscripts $_i$, $_r$, and $_o$ in the definition of the diameter and D and the rotor equivalent wind speed U_{RE}.

In practice, a wind farm simulation with the 3DSL model is divided in blocks, each one dealing with the area within two rows of wind turbines perpendicular to the wind direction, or with the wake of the whole wind farm in case of the last block. The simulation of the first block starts with the evaluation of the wakes outside the induction zone of the turbines in the first row using the near wake model of Sect. 2.5 and stops when the second row of turbines is reached. The simulation of the next block begins with the application of the near wake model to the last wind field cross-section of the previous block. The simulations within the blocks are run on the local stream-wise coordinate x_b, which measures the downstream distance from the beginning of the considered block.

In the application of the near wake model within a wind farm, i.e. downstream the first row of turbines, we consider the wind field on the rotor cross-section as the inflow in the evaluation of the REWS. Doing this we neglect the effect of the induction zone upstream the wind turbine, but this is necessary in order to consider the recovery of the wake. The induction zone, that is the region affected by rotor, begins already in the inflow. For instance the IEC 61400-12-1 standard for power performance measurements suggests to measure the wind speed of the free inflow 2.5 rotor diameters upstream the wind turbine. Power performance measurements exclude the case of wind turbine operating in wakes. We could have followed this indication anyway, but we would have disregard the recovery of the wake. This issue could be solved by recent studies which investigate how to model the induction zone in upstream the wind turbine rotor (Forsting et al., 2016), but it is out of the scope of this work.

3 Model assessment

An evaluation of the 3DSL model is presented in this section, first with regards to the Ainslie model applied to an axisymmetric wake. The 3DSL model is then applied for the simulation of multiple wakes and is assessed using a LES as reference. In the former case the radius and the center-line value of the wake deficit were used as figures of merit. In the latter case, we compared the direct simulation of the interacting wakes by means of the 3DSL model as described in Sect. 2.6 with the quadratic addition of three individual wakes. In this regard, we used the REWS as term of comparison.

Wind Energ. Sci. Discuss., doi:10.5194/wes-2017-1, 2017
Manuscript under review for journal Wind Energ. Sci.
Published: 6 February 2017

eawe european academy of wind energy
Open Access WIND ENERGY SCIENCE DISCUSSIONS

3.1 Model verification on single wakes

To check the consistency of the 3DSL model with the axisymmetric models, we studied six test cases in which we compared the 3DSL model against the Ainslie model implemented in the wind farm layout software *FLaP* (Lange et al., 2003). In this regard, we decided to adopt for both models the near wake model implemented in *FLaP* to initialise the simulations.

3.1.1 The test case

The test cases deal with axisymmetric single wakes of an NREL offshore 5-MW baseline wind turbine (hub height z_H and rotor diameter D of 80 m and 126 m respectively) defined by Jonkman et al. (2009) operating in different atmospheric conditions: A neutral atmospheric stratification, i.e. $\Phi_m(z_H/L_{MO}) = 0$ with three different values of turbulence intensity (TI: 5%, 10% and 15%). For each case, two different hub height inflow conditions (u_H: 8 m/s and 15 m/s) were simulated. The corresponding thrust coefficients (C_T: 0.776, 0.256) were adopted to evaluate the initial wake deficit u_0 $2D$ downstream the rotor (Lange et al., 2003):

$$\begin{aligned} u_0 &= 1 - u_{0_{c-l}} \exp\left(-3.56\left(\tfrac{y}{r^*}\right)^2\right) && \text{where} \\ r^* &= \left(3.56 \tfrac{C_T}{4u_{0_{c-l}}\left(1-0.5u_{0_{c-l}}\right)}\right)^{\frac{1}{2}} && \text{and} \\ u_{0_{c-l}} &= C_T - 0.05 - (16C_T - 0.5)\,0.1\tfrac{TI}{100} \end{aligned} \tag{17}$$

3.1.2 Simulations and results

We evaluated the wake deficit on a 10 D long domain with a 5 D x 5 D cross-section. We used a fixed downstream incremental step in the *FLaP* simulations, providing 17 downstream positions x. Differently, the 3DSL model implements a dynamic step size to ensure the numerical convergence of the solution. The resulting number of downstream positions computed for each test case is listed in Table 1.

Table 1. Test cases and number of downstream positions x calculated with the 3DSL model.

TI [%]	5	5	10	10	15	15
u_H [ms^{-1}]	8	15	8	15	8	15
C_T [-]	0.776	0.256	0.776	0.256	0.776	0.256
N. x	199	147	316	269	437	392

The center-line value u_{c-l} and the corresponding radius r defined as the distance from the rotor axis at which the wake deficit has recovered to 97.17 % (Lange et al., 2003) were chosen as basis for the evaluation and are addressed in Fig. 3. The two models provided very similar results with a maximal discrepancy in the radius of about 0.08 % and of about 0.2 % in the center-line deficit. For the latter, an offset is accumulated until about $x = 3\,D$; afterwards it seems to converge to a constant value. The oscillation of the curves is related to the rougher discretisation of the x axis used in *FLaP*.

Wind Energ. Sci. Discuss., doi:10.5194/wes-2017-1, 2017
Manuscript under review for journal Wind Energ. Sci.
Published: 6 February 2017

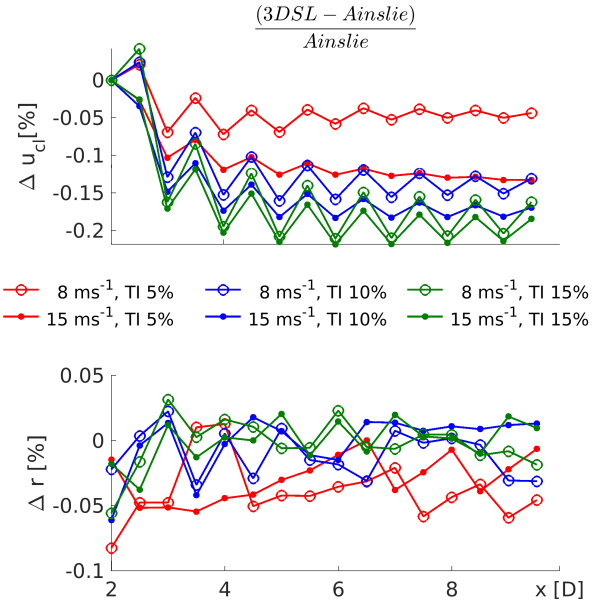

Figure 3. Differences in the downstream development of the center-line deficit (top) and wake radius (bottom) between the Ainslie and the 3DSL model.

3.2 Model evaluation on interacting wakes

To evaluate the advantages provided by the 3DSL model in comparison to the squared addition of the deficits implemented for the simulation of merging wakes in axisymmetric models, we addressed a wind farm including three turbines and compared the two approaches in a benchmark. We decided to consider the case of wake-wake interaction (Fig. 1c) in order to avoid the issue mentioned in Sect. 2.6 about the overlapping of the induction zone in front of the rotor and an upstream wake.

3.2.1 The reference wind field

The reference wind field is calculated with the LES simulation model implemented in PALM (Raasch and Schröter, 2001), coupled with an actuator disc model (Calaf et al., 2010). The case analysed here reproduces three Siemens SWT-2.3-120 wind turbines (120 m rotor diameter D, 90 m hub-height z_H) placed with a consecutive displacement of 6 D downstream and 1.5 D in the cross-stream direction as illustrated in Fig. 4.

The wind field was evaluated on a uniform grid with a spacial resolution of 10 m (0.083 D) and a total domain size of approximately 20 km, 5 km and 3.5 km along the stream-wise, cross-stream and vertical axes respectively. The reference wind field results from the temporal average of 45 min simulated with a time step close to 1 s. With a roughness length $z_0 = 0.002$ m and a vertically constant potential temperature the wind conditions should resemble a typical offshore boundary layer in neutral

Wind Energ. Sci. Discuss., doi:10.5194/wes-2017-1, 2017
Manuscript under review for journal Wind Energ. Sci.
Published: 6 February 2017

eawe european academy of wind energy
Open Access WIND ENERGY SCIENCE DISCUSSIONS

stratification ($\Phi_m(z_H/L_{MO}) = 1$). The hub height inflow 3.3 D upstream the first rotor has a wind speed of 8.26 ms^{-1} with 5 $\%$ turbulence intensity TI.

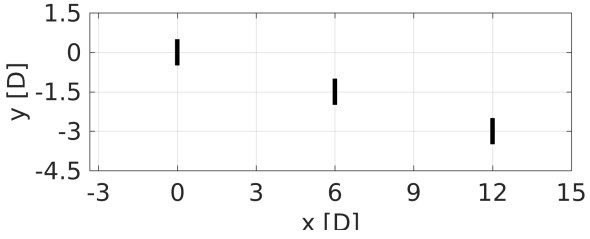

Figure 4. Relative position of the wind turbine rotors within the large eddy simulation domain.

3.2.2 3DSL simulations

We performed two sets of simulations with the 3DSL model using the same inflow condition u_i which was linearly interpolated on a 5 m (0.042 D) grid from the reference wind field at the 3.3 D upstream cross-section (see Fig. 5). The simulation domain covers 20 D in the stream-wise direction, has a cross-strem axis extended form about -7.5 D to 4.2 D and its height exceeds the rotor centre by 3 D.

In the first set of simulations, we reproduced the wake interaction as explained in Sect. 2.6. Three downstream blocks were considered, namely from 2 to 6 D, from 8 to 12 D and from 14 to 20 D.

The second set of simulations involves actually a single run of the 3DSL model from 2 to 20 D downstream the rotor. Three copies of the wake provided as output were located according to the wind farm layout. In the region Ω where the wakes j were overlapping, the wake deficit u_{qs} was estimated with a square addition (Katic et al., 1986; Lange et al., 2003):

$$u_{qs} = \sqrt{\sum_{j\,in\,\Omega} u_j^2} \tag{18}$$

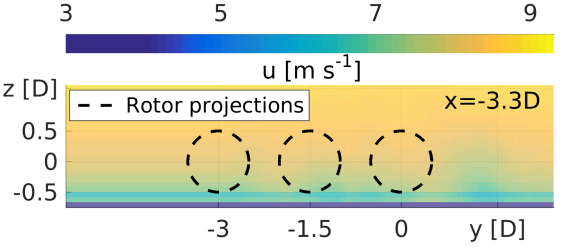

Figure 5. Cross-section of the inflow wind field extracted from the large eddy simulations and used as inflow condition for the 3DSL simulations.

Wind Energ. Sci. Discuss., doi:10.5194/wes-2017-1, 2017
Manuscript under review for journal Wind Energ. Sci.
Published: 6 February 2017

eawe european academy of wind energy
Open Access WIND ENERGY SCIENCE DISCUSSIONS

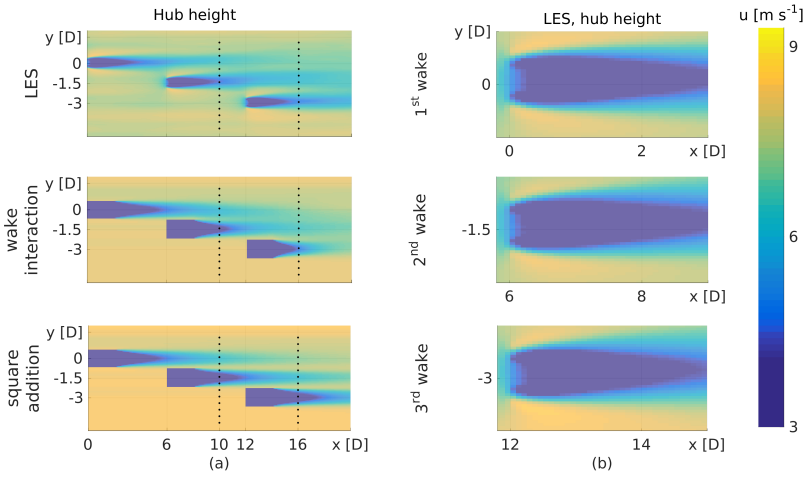

Figure 6. (a) Results of the wind farm simulations on the hub height plane. The black dots indicate the rotor center of the virtual wind turbines used in the assessment of the rotor equivalent wind speed. (b) Zoom on the near wakes on the hub height plane extracted from the large eddy simulations (LES).

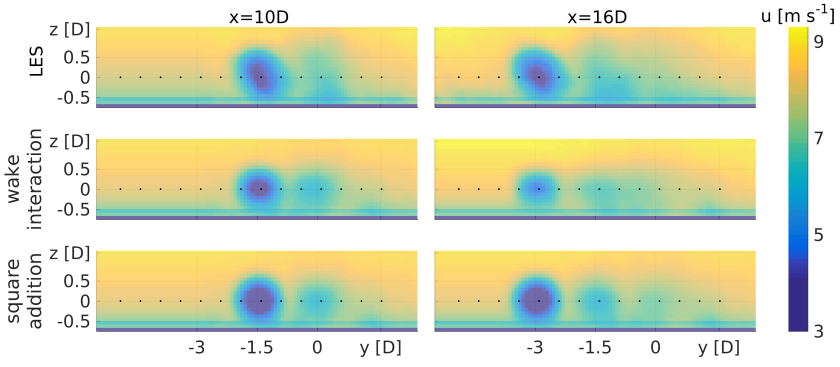

Figure 7. Results of the wind farm simulations on two downstream cross-sections, with two (left) and three (right) wakes. The black dots indicate the rotor center of the virtual wind turbines used in the assessment of the rotor equivalent wind speed.

3.2.3 Results and discussion

The wake interaction and wake superposition simulation results extracted at hub height (Fig. 6a) and at the cross-sections 4 D downstream the second and third rotor (at $x = 6$ and $10\,D$ in Fig. 7 left and right respectively), are qualitatively in agreement with the reference wind field simulated with the LES; however there are some differences. The strongest wakes in the cross-sections of Fig. 7, that is the ones centered at $y = -1.5$ and $-3\,D$ in the top-left and top-right panels respectively, seem to be stretched and slightly rotated in the LES wind field, while this is not the case for the other two simulation approaches. We deem the near wake model to be the reason of this diversity. In fact, from a closer look at the reference wind field at

Wind Energ. Sci. Discuss., doi:10.5194/wes-2017-1, 2017
Manuscript under review for journal Wind Energ. Sci.
Published: 6 February 2017

eawe european academy of wind energy
Open Access WIND ENERGY SCIENCE DISCUSSIONS

hub height (Fig. 6a), the deformation of the wakes appears already in the near wake as an asymmetry with respect to the corresponding rotor axis. The deformation of the wake can be related to the vertical veer of the wind caused by the presence of the Coriolis force. This effect, which is quite small in the present LES, can cause large wake deformations in stable atmospheric stratification (Vollmer et al., 2016). Approaches to consider the wake stretching by wind veer in wake models (Gebraad et al.) are beyond the scope of this paper, but might become more and more relevant with increasing turbine sizes.

As shown in Fig. 6 and in Fig. 7, the wake interaction and wake superposition approaches return very similar results. Maybe there is only a slight difference concerning the interface between merging wakes: With the wake addition approach, the wakes tend to remain separated and merge slower than in the reference wind field. In this respect, the wake interaction approach performs better.

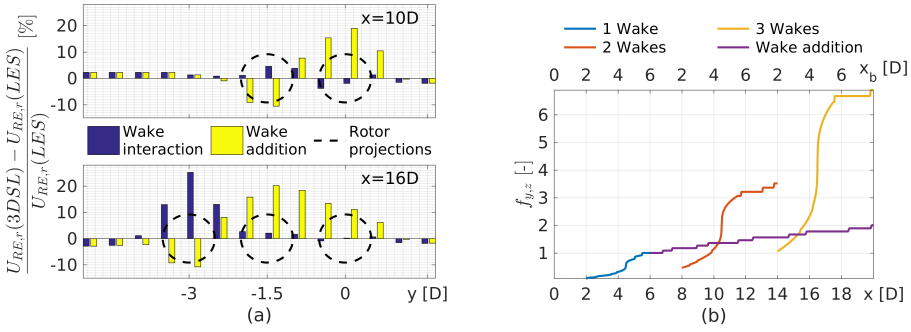

Figure 8. (a) Relative deviation of the rotor equivalent wind speed (REWS) evaluated with the wake interaction and wake addition approaches at the reference cross-sections with respect to the reference wind field (b) Development of the eddy viscosity factor $f_{y,z}$ through the simulation blocks of the wake interaction approach. Here, the bottom and top horizontal axes define the downstream distance from the first upstream turbine (x) and the relative downstream distance within each block of simulation (x_b) respectively.

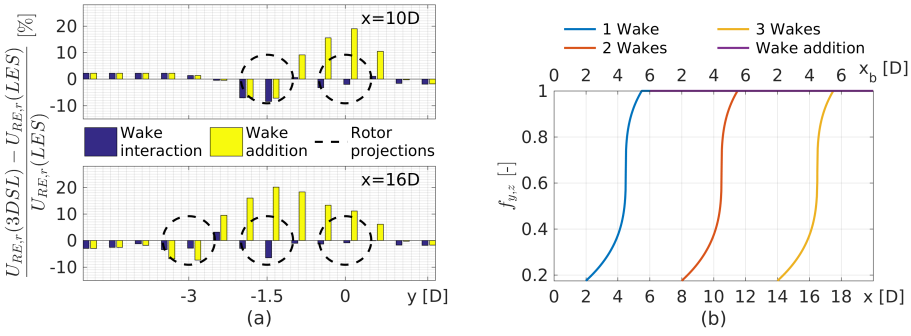

Figure 9. Same as Fig. 8 but using a fixed turbulence mixing length ($r_{y,z}(x) = 1\,D$) in the eddy viscosity model.

Wind Energ. Sci. Discuss., doi:10.5194/wes-2017-1, 2017
Manuscript under review for journal Wind Energ. Sci.
Published: 6 February 2017

eawe european academy of wind energy
Open Access WIND ENERGY SCIENCE DISCUSSIONS

The REWS introduced in Sect. 2.5 can provide a meaningful and more precise assessment of the two multiple wake simulation approaches. In fact, the REWS is a good estimation of the wind turbine operational wind speed from which the thrust acting on the rotor and the power extracted from the wind can be derived. For this analysis we placed a row of 14 virtual units of the same wind turbine type used in the simulations at $x = 10\,D$ and another row at $x = 16\,D$ (black dots in the wind maps of Fig. 6 and of Fig. 7). We did this to evaluate the wake interaction and the wake addition approaches for two and for three wakes. In the former case, the wakes at $y = -1.5\,D$ and $y = 0\,D$ are 10 D and 4 D long. In the latter, 16 D, 10 D and 4 D at $y = -3\,D$, $y = -1.5\,D$ and $y = 0\,D$ respectively.

In the top panel of Fig. 8a, the deviation of the REWS $U_{RE,r}$ calculated from the reference wind field and from the wake interaction simulation at $x = 10\,D$ is always below 5 %. In particular, the REWS is overestimated in the cross-section of the shortest wake (centre at about $y = -1.5\,D$), while it is underestimated in the cross-section of the longest wake (centre at about $y = 0\,D$). The simulations with the wake addition approach provided opposite results with an overall higher deviation with peaks up to 19 %.

In the bottom panel of Fig. 8a, the figure of merit introduced in the previous paragraph refers to the performance of the two simulation approaches for a further downstream section ($x = 16\,D$) including a third wake around $y = -3\,D$. The wake addition method provides results very similar to those of the previous section for the wakes centred around $y = -3\,D$ and $y = -1.5\,D$. We also observe that the deviation from the reference of the REWS within the remaining wakes is lower than at the upstream section.

At the last downstream section ($x = 16\,D$), while a lower deviation from the reference is found for the REWS corresponding to the wake interaction method within the two longest wakes, a very large overestimation (25 %) is observed for the shortest wake. The degradation of these results is linked to the eddy viscosity factor $f_{x,y}$ and more specifically to turbulence length scale $r_{y,z}$.

According to the definition given in Sect. 2.4, $r_{y,z}$ equals the extension of the overall deficit considering all the wakes included on the selected section. When the number of turbines increases, this definition overestimates the turbulence mixing length scale and improperly speeds up diffusion process. The result is a too fast recovery of the wake and an overestimation of the rotor equivalent wind speed.

The problem here is that on a certain cross-section an homogeneous eddy viscosity factor is used to modulate the diffusion at different distances from the rotor generating the wakes. From another perspective, three different values of eddy viscosity are implemented to simulate similar diffusive process at the same downstream distance from the rotor generating the wake.

This issue is well represented in Fig. 8b which illustrates how the eddy viscosity factor evolves downstream through the three blocks of simulations encompassing one (blue line), two (red line) and three (yellow line) wakes respectively. The evolution of the eddy viscosity factor in the wake addition approach (purple line) is included too and it is representative for the case of a single wake.

The same figure also explains why only the REWS values within the wake of the third turbine are overestimated: The blue and red lines assigned to the single and double wake are relatively close around $x = 10\,D$. In this case, the overestimation of the turbulence mixing length is partly compensated by the fact that the filter function slows down the diffusion process of the

Wind Energ. Sci. Discuss., doi:10.5194/wes-2017-1, 2017
Manuscript under review for journal Wind Energ. Sci.
Published: 6 February 2017

wakes from previous blocks of simulations because it is applied to the downstream distance x_b relative to the corresponding simulation block. This mitigating effect is not enough for the wake of the third rotor, whose line at $x = 16\,D$ is significantly more distant from the line representing the single wake (purple line).

To solve the above problem and at the same time to avoid a complex definition of a heterogeneous turbulence mixing length, we decided to fix $r_{y,z}(x) = 1\,D$. We ran the simulations again with this new settings. No significant changes were observed in the results from the wake addition approach. On the contrary, we got remarkable improvements from the wake interaction approach, in particular concerning the REWS within the wake of the third rotor at $x = 16\,D$. In the other cases a minor deterioration of the performances can be observed (see Fig. 9a).

We provide here two possible explanation of the slightly worsening of the results: First, the fixed turbulence mixing length results from the compromise between characteristic turbulence length scales in the intermediate and in the very far wake. An optimization or parametrisation of this value could possibly improve the results. Second, the filter function is still applied to the relative downstream distance within each simulation block. Figure 9b reveals that the incongruity of a homogeneous eddy viscosity factor for different wake conditions on the same cross-section is still unsolved.

4 Conclusions

This paper presents a new non-axisymmetric wake shear layer model (3DSL) that can deal with non-axisymmetric flows and is therefore suitable to directly simulate interacting wakes. It demonstrates that the 3DSL model is equivalent to the commonly used Ainslie model (Ainslie, 1988) implemented for instance in the wind farm layout software *FLaP* (Lange et al., 2003). Furthermore, this study provides a test case which shows how, in terms of rotor equivalent wind speed, the 3DSL model could provide more accurate results than simulation of single wakes combined with a square addition rule.

To allow the simulation of interacting wakes, the 3DSL model abandons the assumptions of an axisymmetric wake implemented for example in the model by Ainslie (1988) and add a third dimension to the simulation domain. In order to do this, it assumes a potential flow on the vertical cross-sections.

The validation against the Ainslie model considered a wind turbine operating at high and low thrust, with different turbulence conditions. The wake radius and center-line deficit resulting from the simulation of the two codes are in agreement with a maximal variation of about 0.08% and 0.21% respectively.

In a benchmark against the large eddy simulations of three interacting wakes, we found that, at two selected cross-sections, the 3DSL model could predict the rotor equivalent wind speed better than the squared addition of single wakes. Some differences from the reference wind field might be linked to the effect of the vertical veer within the atmospheric boundary layer and to the turbulent mixing. An enhanced near wake model and a more detailed description of the eddy viscosity could improve the agreement with the reference.

The proposed model positively passed the first tests and the results indicated the direction to follow for further improvements such that in the near future the simulations of wake interaction within a wind farm could benefit from the purely physical approach adopted in the 3DSL model.

Wind Energ. Sci. Discuss., doi:10.5194/wes-2017-1, 2017
Manuscript under review for journal Wind Energ. Sci.
Published: 6 February 2017

Acknowledgements. This research was carried out in the frame of the RAVE (Research at alpha ventus) research project GW Wakes, funded by the German Federal Ministry for Economic Affairs and Energy (BMWi) based on a decision of the Parliament of the Federal Republic of Germany (grant number 0325397A). Computer resources have been partly provided by the North German Supercomputing Alliance (HLRN) and by the national research project "Parallelrechner-Cluster für CFD und WEA-Modellierung" (FKZ 0325220) funded by the Federal Ministry for Economic Affairs and Energy (BMWi). The authors further want to thank J. Schmidt and J.J. Trujillo for valuable discussions about the content of the manuscript.

Wind Energ. Sci. Discuss., doi:10.5194/wes-2017-1, 2017
Manuscript under review for journal Wind Energ. Sci.
Published: 6 February 2017

eawe european academy of wind energy
Open Access WIND ENERGY SCIENCE DISCUSSIONS

References

Ainslie, J. F.: Calculating the Flowfield in the Wake of Wind Turbines, Journal of Wind Engineering and Industrial Aerodynamics, 27, 213–224, doi:10.1016/0167-6105(88)90037-2, 1988.

Burton, T., Jenkins, N., Sharpe, D., and Bossanyi, E.: Wind Energy Handbook, 2nd Edition, John Wiley & Sons, Ltd., Publication, 2011.

Calaf, M., Meneveau, C., and Meyers, J.: Large eddy simulation study of fully developed wind-turbine array boundary layers, Physics of Fluids, 22, 015 110, doi:10.1063/1.3291077, 2010.

Cebeci, T. and Cousteix, J.: Three-Dimensional Incompressible Laminar and Turbulent Flows, Springer Berlin Heidelberg, 2005.

Crespo, A., Hernández, J., and Frandsen, S.: Survey of modelling methods for wind turbine wakes and wind farms, Wind Energy, 2, 1–24, doi:10.1002/(SICI)1099-1824(199901/03)2:1<1::AID-WE16>3.0.CO;2-7, 1999.

Dyer, A.: A review of flux-profile relationships, Boundary-Layer Meteorology, 7, 363–372, doi:10.1007/BF00240838, 1974.

Forsting, M., Raul, A., Bechmann, A., and Troldborg, N.: A numerical study on the flow upstream of a wind turbine on complex terrain, Journal of Physics: Conference Series, 753, doi:10.1088/1742-6596/753/3/032041, 2016.

Gebraad, P. M. O., Churchfield, M. J., and Fleming, P. A.: Incorporating Atmospheric Stability Effects into the FLORIS Engineering Model of Wakes in Wind Farms, Journal of Physics: Conference Series, 753, 052 004, doi:10.1088/188/1742-6596/753/5/052004.

Jonkman, J., Butterfield, S., Musial, W., and Scott, G.: Definition of a 5-MW Reference Wind Turbine for Offshore System Development, Tech. rep., National Renewable Energy Laboratory, doi:10.2172/947422, 2009.

Katic, I., Højstrup, J., and Jensen, N. O.: A simple model for cluster efficiency, in: EWEC Proc. '86, p. 407–10, http://orbit.dtu.dk/fedora/objects/orbit:66401/datastreams/file_f7da8eb2-e49c-4dc9-9ee5-72846f40ef34/content, 1986.

Keck, R.-E., Veldkamp, D., Madsen, H. A., and Larsen, G.: Implementation of a Mixing Length Turbulence Formulation into the Dynamic Wake Meandering Model, Journal of Solar Energy Engineering, 134, 021 012–021 012, doi:10.1115/1.4006038, 2012.

Lange, B.: Modelling the Marine Boundary Layer for Offshore Wind Power Utilisation, Ph.D. thesis, Carl von Ossietzky Universiät Oldenburg, 2002.

Lange, B., Waldl, H.-P., Guerrero, A. G., Heinemann, D., and Barthelmie, R. J.: Modelling of Offshore Wind Turbine Wakes with the Wind Farm Program FLaP, Wind Energy, 6, 87–104, doi:10.1002/we.84, 2003.

Lissaman, P. B. S.: Energy effectiveness of arbitrary arrays of wind turbines, Journal of Energy, 3, 323–328, doi:10.2514/3.62441, 1979.

Machefaux, E.: Multiple Turbine Wakes, Ph.D. thesis, Technical University of Denmark, 2015.

Madsen, H. A., Larsen, G. C., Larsen, T. J., Troldborg, N., and Mikkelsen, R.: Calibration and Validation of the Dynamic Wake Meandering Model for Implementation in an Aeroelastic Code, Journal of Solar Energy Engineering, 132, 041 014–041 014, doi:10.1115/1.4002555, 2010.

Panofsky, H. and Dutton, J.: Atmospheric Turbulence: Models and Methods for Engineering Applications, John Wiley & Sons Ltd, 1984.

Pope, S.: Turbulent Flows, Cambridge University Press, 2000.

Raasch, S. and Schröter, M.: PALM - A large-eddy simulation model performing on massively parallel computers, Meteorologische Zeitschrift, 10, 363–372, doi:10.1127/0941-2948/2001/0010-0363, 2001.

Vermeer, L, J., Sørsen, J, N., and Crespo, A.: Wind turbine wake aerodynamics, Progress in Aerospace Science, 39, 467–510, 2003.

Vollmer, L., Steinfeld, G., Heinemann, D., and Kühn, M.: Estimating the wake deflection downstream of a wind turbine in different atmospheric stabilities: an LES study, Wind Energy Science, 1, 129–141, 2016.

Wind Energ. Sci. Discuss., doi:10.5194/wes-2017-1, 2017
Manuscript under review for journal Wind Energ. Sci.
Published: 6 February 2017

Walker, K., Adams, N., Gribben, B., Gellatly, B., Nygaard, N. G., Henderson, A., Marchante Jiménez, M., Schmidt, S. R., Rodriguez Ruiz, J., Paredes, D., Harrington, G., Connell, N., Peronne, O., Cordoba, M., Housley, P., Cussons, R., Håkansson, M., Knauer, A., and Maguire, E.: An evaluation of the predictive accuracy of wake effects models for offshore wind farms, Wind Energy, 19, 979–996, doi:10.1002/we.1871, 2016.

Werle, M. J.: Another engineering wake model variant for horizontal axis wind turbines, Wind Energy, pp. 279–299, doi:10.1002/we.1832, 2015.